

01 Jan 2006

Vibration Testing of Repaired Lead-tin/Lead-Free Solder Joints

Matthew O'Keefe

Missouri University of Science and Technology, mjokeefe@mst.edu

S. Vetter

D. Murry

J. Smith

et. al. For a complete list of authors, see https://scholarsmine.mst.edu/matsci_eng_facwork/1456

Follow this and additional works at: https://scholarsmine.mst.edu/matsci_eng_facwork

 Part of the [Materials Science and Engineering Commons](#)

Recommended Citation

M. O'Keefe et al., "Vibration Testing of Repaired Lead-tin/Lead-Free Solder Joints," *Proceedings of the 56th Electronic Components and Technology Conference, 2006*, Institute of Electrical and Electronics Engineers (IEEE), Jan 2006.

The definitive version is available at <https://doi.org/10.1109/ECTC.2006.1645853>

This Article - Conference proceedings is brought to you for free and open access by Scholars' Mine. It has been accepted for inclusion in Materials Science and Engineering Faculty Research & Creative Works by an authorized administrator of Scholars' Mine. This work is protected by U. S. Copyright Law. Unauthorized use including reproduction for redistribution requires the permission of the copyright holder. For more information, please contact scholarsmine@mst.edu.

Vibration Testing of Repaired Lead-Tin/Lead-Free Solder Joints

^a Martin G. Perez, ^a Matthew J. O'Keefe*, ^a Richard Colfax, ^b Steve Vetter, ^b Dale Murry, ^b James Smith,
^c David W. Kleine, ^c Patricia Amick

^a Graduate Center for Materials Research, University of Missouri-Rolla, Rolla, MO 65409 USA, ^b Northrop Grumman Interconnect Technologies, Springfield, MO, ^c Boeing Integrated Defense Systems, St. Louis, MO

* Corresponding author: Tel. 573-341-6764, Fax 573-341-2071, E-mail: mjokeefe@umr.edu

Abstract

Due to growing environmental concerns and recent legislation, tin-lead (Pb-Sn) solders are being phased out by lead-free (LF) solders. The most common Sn-Pb replacement is the tin-silver-copper (Sn-Ag-Cu, SAC) alloys. During the transition phase, it is expected that there will be a period where both Sn-Pb and LF solders will be used side by side, and in conjunction with one another, during assembly processes. Repaired solder joints may also be expected to contain a mixture of Sn-Pb and LF solders, especially in military systems. Very little has been reported on the vibration testing of solder joints in printed circuit boards utilizing LF solders and even less on the vibration testing of solder joints with mixed alloy systems. Aerospace systems typically experience vibration frequencies ranging from the tens of hertz to the thousands of hertz. Given the long life cycle of aerospace vehicles, there exists a need for circuit board repairs and component replacement, which adds to the complexity of the LF transition. Solder joints on these printed circuit boards have a high likelihood of containing a combination of Sn-Pb and LF solders. The vibration fatigue properties of hand-repaired solder joints containing LF solder has not been directly compared with that of hand-repaired Sn-Pb solder joints. Also a correlation between vibration endurance and the solder metallurgy in a repaired joint has not been reported. In this study vibration testing was used to determine how as assembled and repaired Sn-Pb/SAC solder joints withstand dynamic vibration. A frequency sweep from 20Hz to 2000Hz and back down to 20Hz at a constant acceleration of 15g's determined the resonant frequencies of an assembled printed circuit board and its individual components. A 30 minute resonance dwell test at 25 g's determined the vibration resistance of solder joints. The interconnect resistance of the solder joints was measured before and after vibration testing. Tested printed circuit boards were visually inspected for solder cracking and delamination. Metallographic analysis was done on areas where visible cracking or physical damage had occurred. All vibration testing was done at room temperature.

Introduction

Europe, Japan and the United States have begun to replace lead-tin solders (Pb-Sn) with lead-free (LF) solders in consumer products to address environmental and health concerns. These changes are now being implemented in the aerospace industry where avionics are subjected to extreme service conditions. During normal flight operations, avionics experience temperature changes that may range from subzero to well above 25°C. Additionally, avionics experience severe

vibration and shock in service. Adding to the complexity, electronic assemblies may contain a mixture of LF and Sn-Pb solder joints. The difference between Sn-Pb and LF solders cannot always be distinguished, and this may lead to a situation where a Sn-Pb solder joint may be repaired with LF solder.

Vibration testing of solder joints on printed circuit boards (PCB) is not well documented. The vast majority of available literature pertains only to Pb-Sn solder joints. The push for LF solders has resulted in PCBs containing a mixture of Pb-Sn and LF solders (mixed solder systems). The ability of these joints to withstand vibration during flight, take off and landing may not be known. Vibration results from several researchers may help predict how a LF solder joint may withstand vibration or explain how it may fail. However, a direct comparison of lead-free solder versus a lead-tin solder under identical vibration conditions is lacking, especially for hand-repaired solder joints.

The vibration testing of a PCB can be modeled as a single degree of freedom system [1 - 4]. Vibration testing falls into two broad categories: sinusoidal and random. Sinusoidal testing may be used to determine a PCB's resonant frequency and perform a resonance dwell test, a form of fatigue testing. Random vibration can only be predicted on a probability basis, but can better simulate real-world conditions if the vibration profile is known.

For periodic, harmonic excitation, motion may be allowed in the x, y or z-axes. Only in the transverse direction (z-direction or applied force is perpendicular to the PCB) will board bending be most severe [2]. A second order differential equation describes the vibration for a single degree of freedom system [1 - 4]:

$$m(d^2x/dt) + c(dx/dt) + kx = F_0\sin(\omega t) \quad (\text{equation 1}),$$

where m is the mass, c is the damping coefficient, k is the stiffness coefficient, F_0 is the force acting on the mass, ω is the angular velocity in Hertz (Hz), t is time, (d^2x/dt) is the acceleration, (dx/dt) is the velocity, and x is displacement. Vibration testing of a printed circuit board is assumed to be an under-damped case, $\zeta < 1$, where ζ is the critical damping ratio [1, 2, 3, 4]. The natural frequency is given by:

$$\omega_n = (k/m)^{1/2} \quad (\text{equation 2}).$$

For subsonic aircraft, frequencies of 10Hz to 2,000Hz may be experienced during service [5]. Different sources such as the main rotor (11Hz), engine (110Hz), tail rotor (30-60 Hz) and propellers (20+ Hz) contribute to the vibration

spectrum [6]. The natural or resonant frequency of a component may be found by performing a frequency sweep in the range of interest [1 - 4, 7, 8].

Fatigue testing is accomplished by applying acceleration at a PCB's natural frequency. At resonance, large displacements will be experienced and damage will be incurred on the system. For a PCB having a squared or rectangular form, the largest displacement will occur at the center of the PCB at the first mode of vibration [2, 7, 9]. The second and third modes of vibration will have more complicated shapes, but the displacement of the PCB will not be as severe as the first mode [2]. By lowering the stiffness of a component or system, it is possible to achieve lower values of ω_n (equation 2).

The reported failure mechanism behind fatigue failure is the growth of microcracks produced by repeated stress [5]. For example, the corners leads of an inflexible ceramic integrated circuit (IC) package were found to be more prone to failure versus those on the center. The PCB deflected considerably while the ceramic package remained relatively flat at the resonant frequency. The root cause of the failure was a decrease in size of the corner leads after a design change. The smaller lead decreased the component stiffness and greater stresses were experienced.

The stiffness of a material was the most significant factor in simulating how a PCB and ceramic package will perform under vibration tests [5]. Sumikawa et. al reported that the size of a solder ball in a chip scale package is related to its vibration reliability [10]. Larger joints gave longer fatigue life. Cracking was observed in the bulk solder and the interface between the solder and the bond pad. Liu and Ume adjusted the number of solder balls for flip chip components [11]. Missing solder balls on various flip chip samples represented damaged joints. As the number of solder balls decreased, the stiffness of the components dropped. As the number of solder balls in a components dropped, the natural frequency of the component also dropped.

In this investigation, the vibration testing of PCBs containing solder joints with Sn-Pb, LF and a mixture of solder types was conducted. Frequency sweeps determined the PCB resonant frequency, and fatigue tests were performed by doing a frequency locked resonance dwell. The electrical resistance, fatigue resistance, delamination, crack formation and possible microstructural changes were monitored to compare the ability of the solders to withstand sinusoidal vibration.

Procedure

Three test PCBs, measuring 5in. X 6 in., were tested (Figure 1). The PCBs were made of 10 alternating layers of polyimide and copper. An initial layer of hot air solder level (HASL) finish (63/37 SnPb) was present in all PCBs prior to rework. The PCBs contained ball grid arrays (BGAs), 1206 resistors, SO16 SMT and DIP16 through hole components. Each component was internally daisy chained. The BGA components contained no underfill. The first PCB, or control PCB, contained all Sn63/Pb37 components and was tested in the as manufactured condition. The original components from the second and third PCBs were removed and the pads

cleaned with a solder wick. The components were repaired once on the second PCB (R1 for repaired once) and third PCB (MR for multiple repairs). Only the DIP16s were repaired multiple times on the third PCB (MR). The second PCB was selected for scanning electron microscopy (SEM) analysis since it contained different solder combinations (Table 1). Lead-tin (Sn63/Pb37) or LF solder paste (SAC 305 or Sn/3%Ag/0.5%Cu) was applied to select pads on the PCBs. New components containing lead-tinned (Sn63/Pb37) or LF tinned (SAC 305) components were re-flowed and DIP16 components were hand soldered.

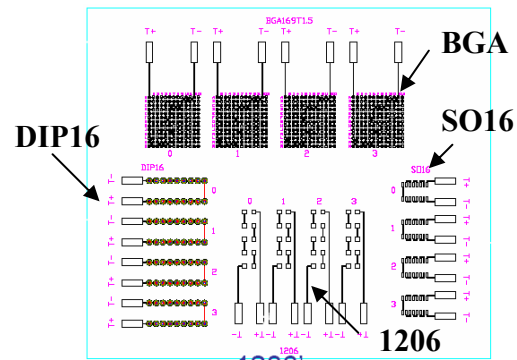


Figure 1: Drawing of PCB that underwent vibration testing.

Table 1: Summary of Repairs for PCBs R1 and MR (L – Lead-tin solder, LF – Lead-free solder)

Part	Position	Solder Paste on Pad	Solder on Component	# Repairs
BGA, 1206, SO16, DIP16*	0	L	L	1
BGA, 1206, SO16, DIP16*	1	L	LF	1
BGA, 1206, SO16, DIP16*	2	LF	L	1
BGA, 1206, SO16, DIP16*	3	LF	LF	1

* - Only DIP16s in PCB MR were hand repaired up to three times.

Vibration testing was undertaken with a MB Dynamics MB-250 electrodynamic exciter (Figure 2). Excitation was applied in the transverse axis with the four corners of the PCB held in place by four aluminum stand-offs. An Endevco I-TEDS accelerometer was placed on the geometric center of the Al base and served as the control accelerometer. An Endevco PE-22 piezoelectric accelerometer that weighed 0.14 grams was placed on the geometric center of the PCB and served as the response accelerometer.

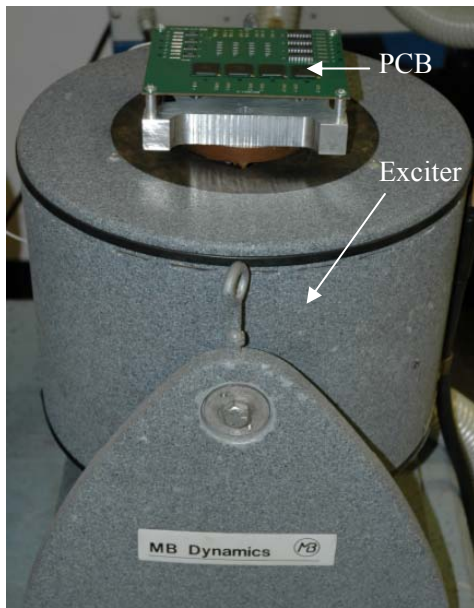


Figure 2: Electrodynamic exciter in vertical position with PCB. Excitation occurs in the transverse direction.

The mechanical vibration tests were based on the IPC-TM-650 standard [12]. All printed circuit boards were cycled through a sine sweep that started from 20Hz, went up to 2000Hz and cycled down to 20Hz in 16 minutes. The acceleration was kept constant at 15g's. LDS Dactron software was programmed to perform the sine sweep while simultaneously searching for the resonant frequencies [8]. Resonant frequencies were calculated by measuring the transmissibilities of the response and control accelerometers. The first mode, or frequency where the PCB exhibited the greatest flexure, was selected for a resonance dwell test at an applied acceleration of 25g's.

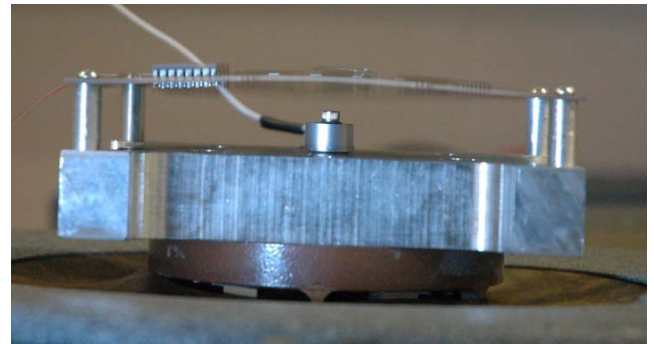
The interconnect resistance of the individual board components was measured using a Quadtech 2000 milliohmeter. Resistance data was collected prior to vibration testing. The resonance dwell test was stopped every five minutes to measure interconnect resistance of individual components. Total test time was 30 minutes. After 30 minutes of testing, a second sine sweep was performed on the boards to measure the changes in resonant frequency. A failure occurred when the interconnect resistance increased by >10% of its initial value or an infinite reading was acquired, which is characteristic of an open circuit.

Components that had electrical shorts were examined for cracks and delamination with a Hyrox KH300 optical microscope. Metallographic specimens were polished up to 0.05µm polishing media and inspected for defects.

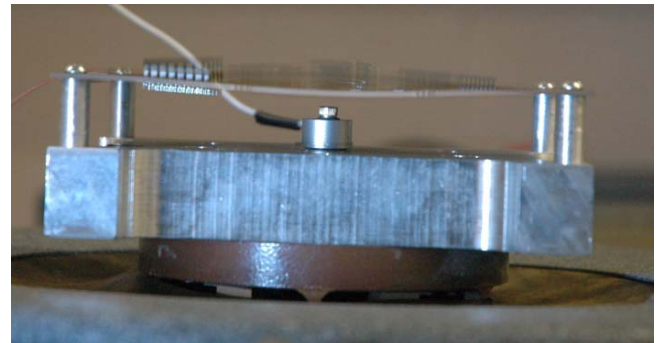
Results

Within the first five minutes of vibration testing, the interconnect resistance for the BGAs and 1206 components and PCB resonant frequency were affected. The initial frequency sweeps showed that the average resonant frequency of the PCBs was ~167Hz. At the first mode, flexure was observed on the middle of the PCBs (Figure 3). Within 25 seconds of starting the resonance dwell, the flexure amplitude

was observed to drop to about 50-66% of its initial level. After a 30 minute cumulative resonance dwell, the average resonant frequency dropped to ~160Hz.



A.

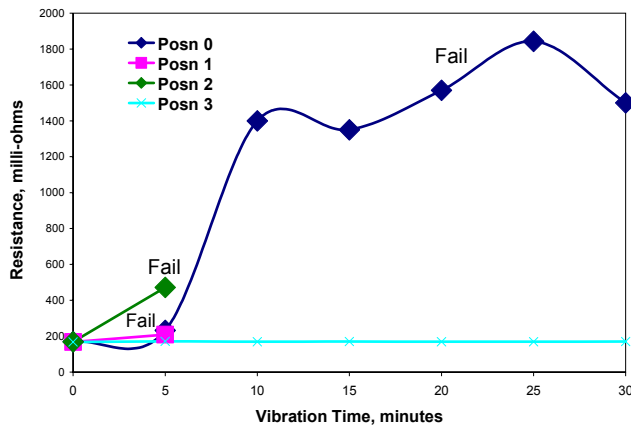


B.

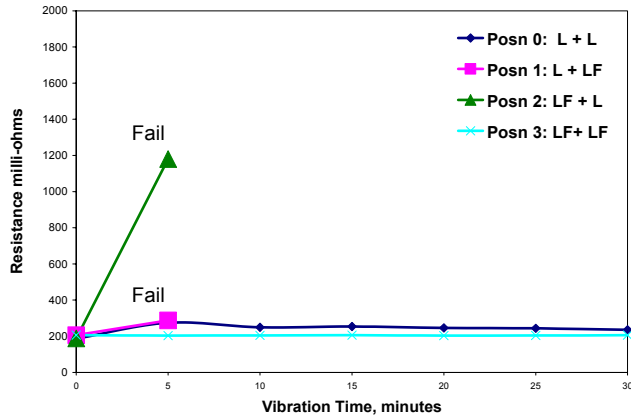
Figure 3: PCB at first mode of vibration. The resonant frequency is ~167Hz.

The interconnect resistance of the SO16 and DIP16 components remained constant; no opens were detected during vibrations testing. This implied that Sn-Pb, LF and mixed solder components performed equally well under sinusoidal vibration testing.

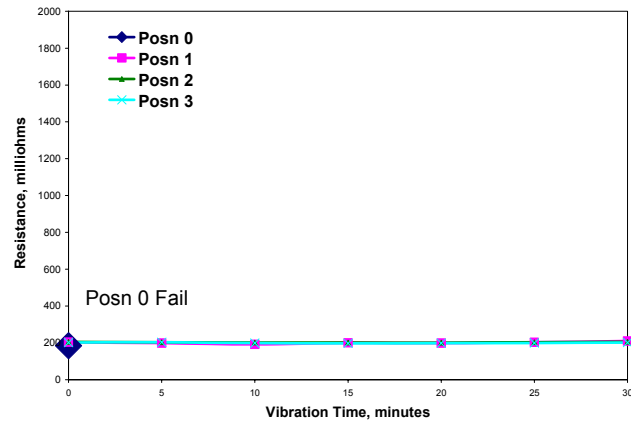
Opens were detected on the BGAs after the first five minutes of the resonance dwell. The BGAs were the first component to fail. This resulted in a drop in PCB resonant frequency, which was most likely caused by an overall drop in board stiffness. Failures or interconnect opens for the 1206 components were more likely to occur for the center components or positions 0, 1 and 2 (Figure 4 and Figure 1). Optical images for the failed 1206 components showed cracking in the bulk solder or delamination of the component from the solder (Figure 5).



A. Control PCB – All Pb-Sn solder joints

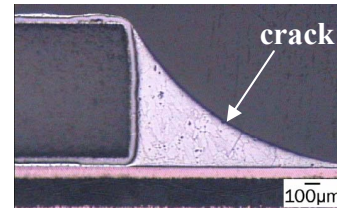


B. PCB R1 – L= Pb-Sn, LF = lead-free solder

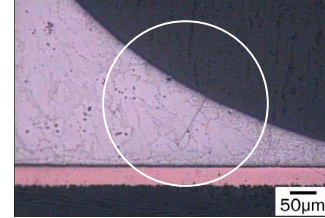


C. PCB MR – All LF solder joints, except 0 (Pb-Sn)

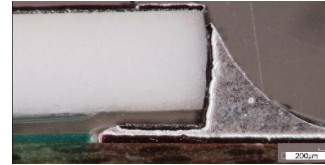
Figure 4: Interconnect Resistance for 1206 components during a resonance dwell test. Bold symbols represent open circuit.



A. 1206 Component #1 with crack: PCB R1

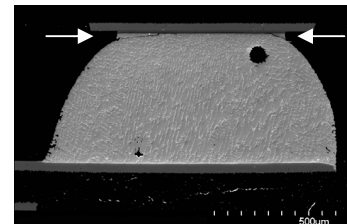


B. Detail of crack in solder.

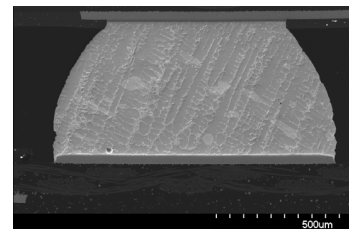


C. Delamination of 1206 component #2: CONTROL PCB
Figure 5: Damage in 1206 components.

Edge balls or balls adjacent to the edge or corners of the BGA were likely to fail by cracking while the middle solder joints remained intact (Figure 6). This trend was observed for all BGAs regardless of solder type (Figures 7 and 8). The crack started at the region of the solder ball where the solder mask is applied. This region corresponds to the smallest diameter of the ball. The crack started on the outside and traveled into the solder bulk. This behavior was not always consistent since it was also possible for the crack to propagate into the intermetallic layer formed between the solder and the component pad (Figure 8A). The damaged was caused by higher tensile and compressive stresses experienced by the edges and corners of a BGA component as the PCB deflects during the first mode of vibration (Figure 9).

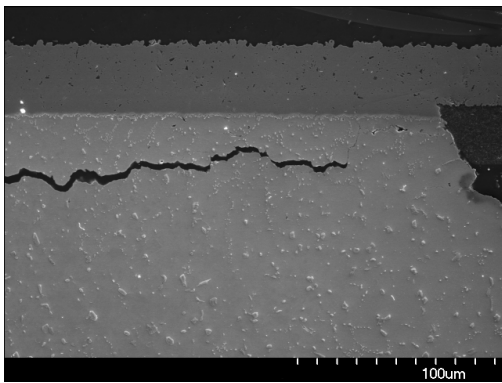


A. Edge solder ball with crack (arrows).

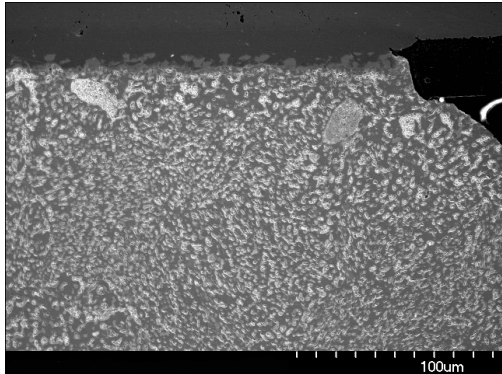


B. Middle solder ball.

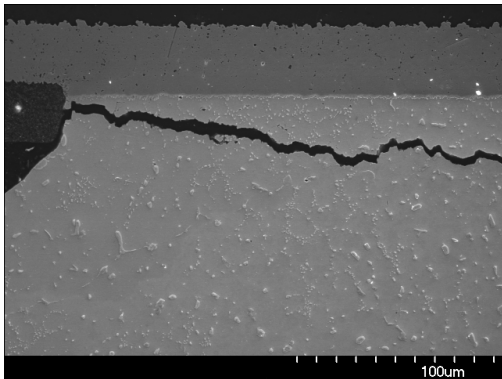
Figure 6: BGA solder balls for CONTROL PCB (100X).



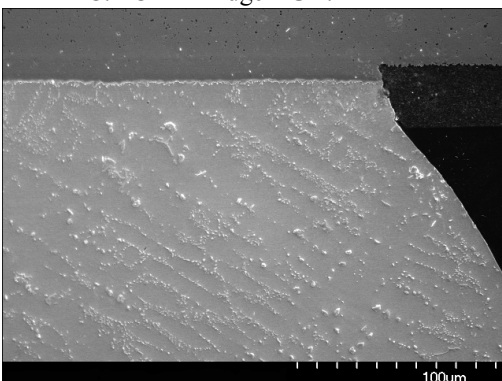
A. PCB R1 Edge BGA: L + L



B. PCB R1 Middle BGA: L + L

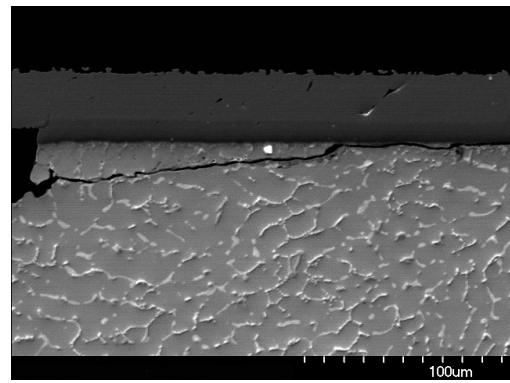


C. PCB R1 Edge BGA: LF + LF

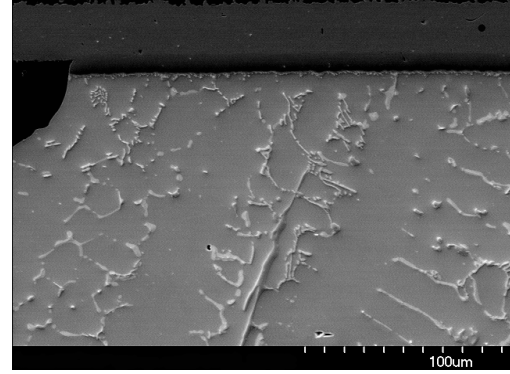


D. PCB R1 Middle BGA: LF + LF

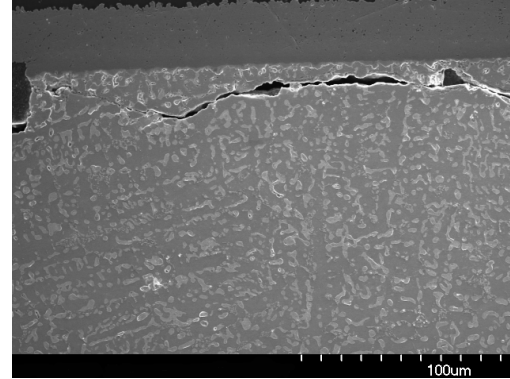
Figure 7: SEM images (500X) of BGAs where the solder mask was applied. First letter corresponds to type of solder paste on pad and the second to solder type on the component.



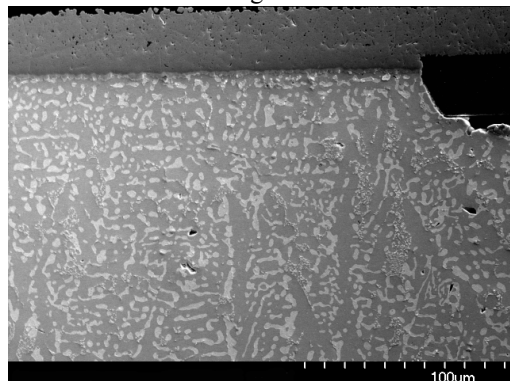
A. PCB R1 Edge BGA: L + LF



B. PCB R1 Middle BGA: L + LF



C. PCB R1 Edge BGA: LF + L



D. PCB R1 Middle BGA: LF + L

Figure 8: SEM images (500X) of BGAs where the solder mask was applied. First letter corresponds to type of solder paste on pad and the second to solder type on the component.

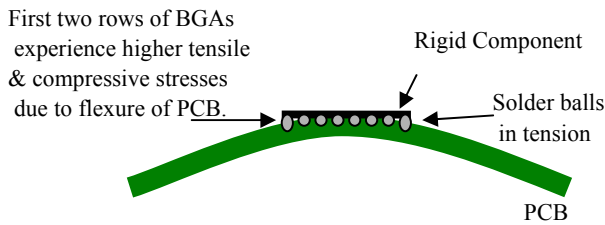


Figure 9: Exaggerated flexure of PCB and its effect on a BGA component at first mode of vibration.

Conclusions

Initial vibration test results showed that different types of solder had comparable performances during vibration testing. Interconnect failure was due more to component location rather than solder type or repair for BGA and 1206 components. The 1206 components located closer to the center experienced greater flexure and failed. All BGAs failed within the first 5 minutes of testing. The BGA components were centrally located within the PCB without underfill, and this may have accelerated the failures. The corner and edge solder balls in BGAs experienced greater flexure than those in the middle. Failure may be an effect of the small amount of solder used on the BGA and 1206 components. The larger components had greater amounts of solder, and all had comparable interconnect resistance and no failures after 30 minutes of vibration testing.

The drop in resonant frequency was attributed to a drop in PCB stiffness, k , as a result of testing (i.e. $\omega_n = (k/m)^{1/2}$). After breaking solder joints, the BGAs contributed less to the overall PCB stiffness.

The cause of interconnect resistance failures was attributed to cracks in the solder or delamination. Cracking in the BGAs was attributed to fatigue damage that started at the solder mask region on the surface of the BGA. The crack propagated in the matrix or the intermetallic layer between the solder and component pad.

There was insufficient data to detect possible effects on the microstructure after vibration testing. The resonance changed after a few minutes. Future vibration testing will incorporate a frequency tracked resonance dwell instead of a frequency locked dwell test. This will impart greater stress to the larger solder joints for longer periods of time.

Acknowledgments

This work was funded through the Materials and Manufacturing Directorate of the Air Force Research Laboratory (AFRL) at Wright-Patterson AFB, OH, contract FA8650-04-C-704. The support of AFRL program managers Dr. Mary Kinsella, Dr. Jay Tiley, and Lt. Kacey Blunck is gratefully acknowledged. Technical guidance and advice of David Johnson and Larry Perkins at AFRL is also acknowledged. A special thank you goes to Kenny Allison, Ron Haas, and Jeff Wight for help setting up the vibration test equipment and to Vanessa Eckhoff and Ken Doering for the metallographic work and optical images.

References

1. Rao, Singiresu S., *Mechanical Vibrations*, 4th ed., Pearson-Prentice Hall, 2004.
2. Tustin, Wayne, *Vibration Testing and Screening of PCBs*, May 6, 2003, www.vibrationandshock.com/course5.htm,
3. Inman, Daniel J, *Engineering Vibration*, 2nd ed., Prentice Hall, 2001.
4. Pennington, Dale, *Basic Shock and Vibration Theory*, Endeveco Technical Paper, 219, Revised 2/74, www.endevco.com.
5. Grimes, Jeanne, 72nd Air Base Wing Public Affairs, Lab Uses Vibration Testing to Solve Aircraft Problems, *Air Force Print News Today*, May 23, 2005, af.mil/news.
6. *Vibration in aviation*, usuhs.mil/mim/NoiseVibration%20Notes.doc.
7. Morgen, Richard J., *Vibration Screening Catches Early IC Failures*, *Machine Design*, October 10, 1994, pp. 113-114.
8. LDS Dactron Shaker Control User Guide V5.0, LDS Group Company, 2002
9. Ramakrishnan, Aru and Pecht, Michael G., *A Life Consumption Monitoring Methodology for Electronic Systems*, *IEEE Transactions and Components Packaging Technologies*, Vol. 26, NO. 3, June 2003, pp. 625-634.
10. Sumikawa, Masato, et. al, *Reliability of Soldered Joints in CPPs of Various Designs and Mounting Conditions*, *IEEE Transactions and Components Packaging Technologies*, Vol. 24, NO. 2, June 2001, pp. 293-299.
11. Liu, Sheng and Ume, Charles, *Vibration Analysis Based Modeling and Defect Recognition for Flip-Chip Solder-Joint Inspection*, *Journal of Electronic Packaging*, September 2002, Vol. 124, pp. 221-226.
12. IPC-6012 Standard, IPC-TM-650 Test Methods Manual, *Rigid Printed Wiring Vibration*, No. 2.6.9, 8/97, Rev. A.